AGU100 ADVANCING EARTH AND SPACE SCIENCE

Geophysical Research Letters

RESEARCH LETTER
10.1029/2018GL077597

Special Section:
The Three Major Hurricanes of 2017: Harvey, Irma and Maria

Increasing Magnitude of Hurricane Rapid Intensification in the Central and Eastern Tropical Atlantic

Karthik Balaguru[1], **Gregory R. Foltz**[2], **and L. Ruby Leung**[3]

[1]Marine Sciences Laboratory, Pacific Northwest National Laboratory, Seattle, WA, USA, [2]Physical Oceanography Division, Atlantic Oceanographic and Meteorological Laboratory, Miami, FL, USA, [3]Atmospheric Sciences and Global Change, Pacific Northwest National Laboratory, Richland, WA, USA

Abstract Rapid intensification (RI) of hurricanes is notoriously difficult to predict and can contribute to severe destruction and loss of life. While past studies examined the frequency of RI occurrence, changes in RI magnitude were not considered. Here we explore changes in RI magnitude over the 30-year satellite period of 1986–2015. In the central and eastern tropical Atlantic, which includes much of the main development region, the 95th percentile of 24-hr intensity changes increased at 3.8 knots per decade. In the western tropical Atlantic, encompassing the Caribbean Sea and the Gulf of Mexico, trends are insignificant. Our analysis reveals that warming of the upper ocean coinciding with the positive phase of Atlantic Multidecadal Oscillation, and associated changes in the large-scale environment, has predominantly favored RI magnitude increases in the central and eastern tropical Atlantic. These results have substantial implications for the eastern Caribbean Islands, some of which were devastated during the 2017 hurricane season.

Plain Language Summary In this study, using an analysis of observations and climate model output, we demonstrate that the magnitude of rapid intensification (RI), defined as an event where a hurricane increases in intensity by 25 knots or higher in 24 hr, increased in the central and eastern tropical Atlantic during the 30-year satellite period of 1986–2015. On the other hand, in the western tropical Atlantic, changes in RI magnitude are insignificant. Conspiring changes in the large-scale hurricane environment brought about by a positive shift in the phase of the Atlantic Multidecadal Oscillation, the dominant mode of decadal climate variability in the Atlantic, are primarily responsible for these changes in RI. While previous studies examined the frequency of RI, our study is the first to understand potential changes in RI magnitude. The results from our study have substantial implications for the eastern Caribbean Islands, some of which were ravaged by several major hurricanes undergoing RI during the recently concluded 2017 Atlantic hurricane season.

Key Points:
- Magnitude of hurricane rapid intensification had increased in the central and eastern tropical Atlantic
- Changes in the large-scale hurricane environment are responsible for these changes in hurricane rapid intensification
- A positive shift in the Atlantic Multidecadal Oscillation caused the environment to become more favorable for hurricane rapid intensification

Supporting Information:
- Supporting Information S1

Correspondence to:
K. Balaguru,
Karthik.Balaguru@pnnl.gov

Citation:
Balaguru, K., Foltz, G. R., & Leung, L. R. (2018). Increasing magnitude of hurricane rapid intensification in the central and eastern tropical Atlantic. *Geophysical Research Letters*, *45*, 4238–4247. https://doi.org/10.1029/2018GL077597

Received 15 FEB 2018
Accepted 2 APR 2018
Published online 3 MAY 2018

1. Introduction

Rapid intensification (RI) of hurricanes is difficult to forecast and consequently poses significant operational challenges (Elsberry, 2014; Emanuel, 2017a; Lee et al., 2016; Rappaport et al., 2012; B. Wang & Zhou, 2008; C. Wang et al., 2017). Despite its relatively rare occurrence, RI has an important impact on the climatological probability distribution of hurricane intensities (Lee et al., 2016). RI played a prominent role during the recently concluded hyperactive 2017 Atlantic hurricane season, which was the costliest on record for the United States (Rahmstorf, 2017). Out of a total of 17 named tropical storms that formed, 10 developed into hurricanes and 6 achieved major hurricane status. Four hurricanes reached Category 4 or 5 strengths (Harvey, Irma, Jose, and Maria). Hurricane Harvey rapidly intensified in the northern Gulf of Mexico before making landfall near Rockport, Texas, on 26 August and produced record levels of rainfall in the Houston metropolitan area (Emanuel, 2017b). Irma underwent RI in the eastern tropical Atlantic during late August and early September before achieving Category 5 strength and maintaining that intensity for a record amount of time (Rahmstorf, 2017). Hurricane Jose, which achieved a peak intensity of Category 4, went from a tropical storm to a major hurricane in the central tropical Atlantic in less than 2 days between 6 and 8 September. Finally, Hurricane Maria, which made devastating landfalls in Dominica and Puerto Rico at Category 5 and 4 strengths, respectively, underwent a phase of RI between 16 and 18 September in a region to the east of the islands of Lesser Antilles (Zorrilla, 2017).

The evolutions of the storms in 2017 are consistent with the observation that nearly all Category 4 and 5 Atlantic hurricanes undergo RI at some stage during their lifetime (B. Wang & Zhou, 2008), but there is one interesting point to note. For the climatological mean RI, the probability of occurrence is higher in the Gulf of Mexico and the Caribbean Sea and is relatively low in the central and eastern tropical Atlantic (CETA; C. Wang et al., 2017). However, three of the four hurricanes that reached at least Category 4 strength in 2017 underwent RI in the latter. It is important to know whether the events of 2017 are a short-term aberration or part of a longer-term trend. This leads to the following questions: Have the characteristics of hurricane RI been changing in the CETA (defined as the region between 60°W–10°W and 10°N–20°N), or the western tropical Atlantic (WTA: defined as the region between 100°W–60°W and 10°N–30°N)? If so, can we identify corresponding changes in the large-scale hurricane environment? To address these, we perform an analysis of hurricane track data and ocean-atmosphere conditions in the Atlantic for the 30-year satellite period of 1986–2015. In section 2, we describe the data and methods used in our analysis. The results are explained in section 3, and finally, a discussion of the main conclusions and their implications is given in section 4.

2. Data and Methods

2.1. Data

Hurricane track and intensity data for the 30-year satellite period of 1986–2015 were obtained from National Oceanic and Atmospheric Administration (NOAA)'s Atlantic Hurricane Database 2 (http://www.aoml.noaa.gov/hrd/hurdat/Data_Storm.html; Landsea et al., 2015). This data set provides 1-min averaged sustained winds at an elevation of 10 m. These data were used to find hurricane track locations and estimate hurricane intensification rates. In addition to data from the 30-year period, data for the 2016 hurricane season were also obtained from Hurricane Database 2 to denote RI locations in Figure 2. However, hurricane track locations and along-track intensities for hurricanes Harvey, Irma, Jose, and Maria from the 2017 season, also used in Figure 2, were based on preliminary estimates.

Sea surface temperature (SST) data from NOAA, obtained from http://www.emc.ncep.noaa.gov/research/cmb/sst_analysis/, are used to compute trends in SST (Reynolds et al., 2002). Subsurface temperature profiles from the Hadley Center's EN4 data (Good et al., 2013), obtained from https://www.metoffice.gov.uk/hadobs/en4/, are used to compute tropical cyclone heat potential (TCHP). The data here have been compiled using an objective analysis of all available hydrographic measurements including Argo. Atmospheric temperature and relative humidity, zonal and meridional winds, and sea level pressure (SLP) data from National Centers for Environmental Prediction-2 reanalysis (Kanamitsu et al., 2002), available at https://www.esrl.noaa.gov/psd/data/gridded/data.ncep.reanalysis2.html, were also obtained. Atmospheric temperature, relative humidity, and SLP data are combined with SST data to compute potential intensity (PI), based on Emanuel (1999). Relative humidity data are used to examine trends in midtropospheric humidity. Horizontal winds are used to estimate vertical wind shear (VWS) and upper-level divergence. To validate the results based on these data sets, we carried out similar analysis using SST data from the UK Met Office Hadley Center (Rayner et al., 2003) (https://www.metoffice.gov.uk/hadobs/hadisst/), subsurface temperature profiles from National Centers for Environmental Prediction Global Ocean Data Assimilation System (Behringer & Xue, 2004) (http://www.esrl.noaa.gov/psd/), and ERA-interim atmospheric reanalysis data (Dee et al., 2011; https://www.ecmwf.int/en/forecasts/datasets/reanalysis-datasets/era-interim). All data used are at monthly mean resolution for the period 1986–2015 and for the months of August–October.

Monthly time series of Atlantic Multidecadal Oscillation (AMO), El Niño–Southern Oscillation (ENSO), and North Atlantic Oscillation (NAO) climate indices were obtained for the period 1986–2015 from https://climexp.knmi.nl/start.cgi. The monthly Atlantic Meridional Mode (AMM) index was obtained for the same period from https://www.esrl.noaa.gov/psd/data/timeseries/monthly/AMM/. The AMO index is calculated as SST averaged over the North Atlantic between 0–60°N and 80°W–0, and with the SST averaged globally between 60°S and 60°N removed from it (Trenberth & Shea, 2006). To diagnose ENSO events, we use the Multivariate ENSO Index, which combines the characteristics of all observed surface variables in the tropical Pacific, including SST (Wolter & Timlin, 1998). The NAO index is estimated as the principal component time series of the leading empirical orthogonal function of winter SLP anomalies over the North Atlantic between 90°W–40°E and 20°N–80°N (Hurrell, 1995). Following Chiang and Vimont (2004), the AMM index is estimated based on a maximum covariance analysis applied to SST and surface wind fields in the Atlantic between 75°W–15°E and 20°S–30°N. The SST expansion coefficient is used as the index in our study. While the AMO,

ENSO, and AMM indices are averaged over August–October, the NAO index is averaged over January–March (C. Wang et al., 2017).

Monthly mean SST and winds from climate models belonging to the Intergovernmental Panel on Climate Change's Coupled Model Intercomparison Project phase 5 (CMIP5) were obtained from the Earth System Grid Federation at https://esgf-node.llnl.gov/projects/esgf-llnl/ and are used to examine trends associated with global warming in SST and VWS. Sixteen models from climate centers across the world are used (Masson & Knutti, 2011). Data are obtained for the 30-year period 1986–2015 and from a single ensemble member for each model. Data from historical simulations are used for the period 1985–2005, and data from Representative Concentration Pathway 8.5 emissions scenario are used for the period 2006–2015. The models used are the following: ACCESS1.3, BCC-CSM1.1, CanESM2, CESM1 (CAM5), CMCC-CM, CNRM-CM5, CSIRO-Mk3.6.0, GFDL-ESM2G, GISS-E2-H, HadGEM2-ES, INM-CM4, IPSL-CM5A-LR, MIROC5, MPI-ESM-MR, MRI-CGCM3, and NorESM1-ME.

2.2. Methods

2.2.1. Trends in Upper Quantiles of Intensification Rates

For both WTA and CETA, we generate time series of upper quantiles of 24-hr intensity changes. The WTA includes the Gulf of Mexico, Caribbean Sea, and a small region to the east of Florida in the open Atlantic, while the CETA is essentially the hurricane main development region except the Caribbean Sea. In each subregion and for each hurricane season, we compute the value of the 95th percentile of 24-hr intensity changes based on all 6-hourly track locations. Note that on average, the 95th percentile of 24-hr intensity changes corresponds to RI (Kaplan & DeMaria, 2003; Kaplan et al., 2010). Also, using this approach allows us to generate a continuous time series irrespective of the maximum intensification rate attained in either subregion for a given season.

2.2.2. Changes in RI Magnitude

To compute the mean change in RI magnitudes, we use the "Monte Carlo" technique of repeated random selection. For both WTA and CETA, we first develop two subsets of RI magnitudes. The first subset has all RI magnitudes for the first 15-year period of 1986–2000 in the subregion, while the second subset has RI magnitudes for the second 15-year period of 2001–2015. Note that RI is defined as an increase in intensity of at least 25 knots in 24 hr. Next, we randomly select approximately half of the RI samples from each subset. From the randomly selected samples, we again subsample such that no two RI locations are within 24 hr of each other. A spatiotemporal autocorrelation analysis (supporting information, Figure S1) reveals that the correlation between 24-hr intensity changes drops below 0.2 when the samples are at least 24 hr apart. In other words, less than 5% of the variance in intensity change 24 hr later is explained by intensity change at the current location along hurricane tracks. Hence, to ensure that the randomly selected samples are independent, we further subsample the randomly selected samples such that no two RI locations are within 24 hr of each other. We then compute the mean value for each group of RI magnitudes resulting from the two rounds of subsampling described above, and we also compute the t value corresponding to a Student's t test for difference of means for the two RI groups. We repeat this whole process 1,000 times and generate 1,000 values of mean RI magnitudes for each 15-year period and 1,000 t values for each subregion. The final value of mean RI magnitude for each 15-year period and the t value for statistical significance for each subregion are given by the mean of those 1,000 values.

2.2.3. Trends in RI Occurrence

To understand changes in RI occurrence, we generate an RI fraction time series. For each subregion, we estimate the fraction of 6-hourly track locations where RI has occurred in each hurricane season, unlike some previous studies (C. Wang et al., 2017) where the actual number of RI events per season was used. Besides providing a continuous time series for calculation of trends, our approach also normalizes RI frequency with the total number of 6-hourly hurricane track locations and, consequently, provides a more realistic picture of changes in RI occurrence with time.

2.2.4. Environmental Parameters That Impact RI

PI (Emanuel, 1999) is a representation of the hurricane's thermodynamic environment. It is the theoretical limit to the maximum possible intensity that a hurricane can attain under the prevailing conditions. Using SST, SLP, and vertical atmospheric profiles of temperature and relative humidity, PI is calculated as follows:

$$\mathrm{PI}^2 = \frac{C_k}{C_d}\frac{\mathrm{SST}-T_o}{T_o}(k_s-k_a), \quad (1)$$

where C_k and C_d are the coefficients of enthalpy and drag, respectively, T_o is the outflow temperature, and k_s and k_a are the specific enthalpies of air at the air-sea interface and in the ambient boundary layer. The program to compute PI is available at http://eaps4.mit.edu/faculty/Emanuel/products. TCHP (Leipper & Volgenau, 1972), a representation of the upper-ocean heat content relevant for hurricane intensification, is estimated as the integral of the ocean temperature from the surface to the depth of the 26°C isotherm as follows:

$$\mathrm{TCHP} = \int_0^{Z_{26}} \rho\, C_p\, (T(z) - 26)\, \mathrm{d}z, \tag{2}$$

where Z_{26} is the depth of the 26°C isotherm, C_p is the specific heat capacity of seawater, and $T(z)$ is the temperature of the ocean as a function of depth. VWS is estimated as the vertical difference of the horizontal winds between the 200- and 850-hPa levels (Kaplan & DeMaria, 2003). Finally, while trends in divergence are computed at the 200-hPa level (Kaplan et al., 2010), relative humidity trends are examined at the 500-hPa level (Shu et al., 2012; C. Wang et al., 2017).

The impact of AMO on various environmental parameters that influence hurricane RI is estimated using a semipartial correlation analysis. First, we correlate the time series of a given environmental parameter, area averaged over a region, with the time series of the 95th percentile of 24-hr intensity changes for that region. Next, we compute the correlation between the quantile time series and the time series of the environmental parameter after removing the influence of AMO from that parameter. In other words, we correlate the quantile time series with the residual obtained after removing the regression of the environmental parameter on AMO. If the original correlation coefficient is statistically significant and the correlation coefficient after accounting for AMO is statistically insignificant, we conclude that AMO is the main driver of the relationship between that environmental parameter and the quantile time series.

2.2.5. Effect of Global Warming on the Tropical Atlantic Hurricane Environment

To decouple the influence of global warming on the large-scale hurricane environment from that of natural variability, we examine ensemble mean trends from climate model output. Since natural variability, such as the AMO, occurs in different phases in different models, they tend to cancel when averaged across the models, leaving only the response to external forcing in the ensemble mean (Meehl et al., 2014). To compare the spatial pattern of SST trends found in observations with that simulated in models, we use the method of pattern correlation. Following Smith et al. (1994), the number of spatial degrees of freedom used to estimate the significance of the pattern correlation coefficient is calculated as

$$\text{Degrees of freedom} = \frac{N \sum_{i=1}^{N} \sigma_i^2}{\sum_{i=1}^{N} \sigma_i^2 + 2 \sum_{i=1}^{N-1} \sum_{j=i+1}^{N} \mathrm{Cov}_{i,j}}, \tag{3}$$

where σ_i^2 is the variance of SST at each ith grid point, $\mathrm{Cov}_{i,j}$ is the pair-wise covariance for SST between the ith and jth grid points, and N is the total number of grid points with SST. Using the monthly mean NOAA SST data set, we estimate the number of spatial degrees of freedom for SST to be 11.

3. Results

3.1. Changes in Hurricane Intensification Rates

We begin by examining trends in quantiles of 24-hr hurricane intensity changes (see section 2.2). The use of quantiles or percentiles to define the threshold of intensity changes ensures that we have a continuous time series of values irrespective of the distribution of intensity changes for a given hurricane season, allowing us to perform trend analysis. Trends in the 50th percentile of 24-hr intensity changes are statistically insignificant in the WTA (Figure 1a) and the CETA (Figure 1b), suggesting that there has not been a significant change in the median intensification rates. But, results are different when upper quantiles are considered. In the WTA, even the trend in the 95th percentile values is statistically insignificant (Figure 1a). However, in the CETA, the trend in the 95th percentile of 24-hr intensity changes is 3.8 knots per decade, a value statistically significant at the 95% level (Figure 1b). Since the 95th percentile of 24-hr intensity changes roughly corresponds to RI (Kaplan & DeMaria, 2003; Kaplan et al., 2010), the positive linear trend probably indicates that the RI magnitude has increased in the CETA over that period.

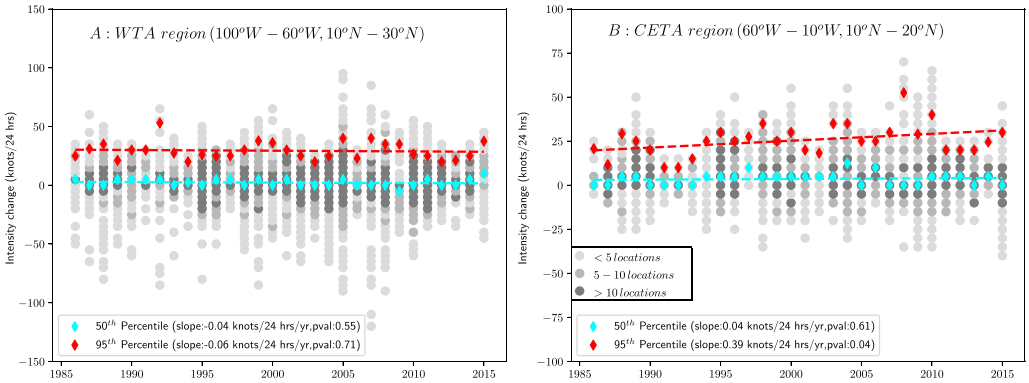

Figure 1. Observed trends in quantiles of 24-hr intensity change over the 30-year period 1986–2015 for (a) western tropical Atlantic (WTA) and (b) central and eastern tropical Atlantic (CETA). In panels (a) and (b), gray circles denote the 24-hr intensity change values at various 6-hourly hurricane track locations for each season, with darker shades of gray indicating more locations with that value of intensity change (see legend). The median quantile value and the value of 95th percentile for each season are denoted by cyan and red diamonds, respectively. Trends in time series of median quantile and the 95th percentile of 24-hr intensity changes are also shown. The slopes of the trend lines and the *p* values for statistical significance of those trend lines are provided (see legend).

To understand this further, we consider changes in RI magnitude. Although the most commonly used definition of RI is an intensity change of 30 knots or higher in 24 hr (Kaplan & DeMaria, 2003; B. Wang & Zhou, 2008; C. Wang et al., 2017), a minimum intensity change of 25 knots in 24 hr has also been used (Kaplan et al., 2010; Klotzbach, 2012; Sampson et al., 2011). We use the latter threshold to define RI in our study because it increases the sample size for our analysis. The RI locations (Figure 2) are consistent with the regions of warmest climatological SST in the Atlantic: RI tends to be stronger and occurs more frequently in the WTA than in the CETA (C. Wang et al., 2017). The mean RI magnitude in the CETA during the first 15-year period 1986–2000 is 28.3 knots per 24 hr and during the second 15-year period 2001–2015 is 31.2 knots per 24 hr. These values were generated based on the Monte Carlo technique of repeated random sampling (see section 2.2) while taking into account the number of degrees of freedom along each storm track, as described below.

It can be seen from Figure 2 that RI locations tend to occur in clusters along hurricane tracks. A spatiotemporal autocorrelation analysis (see section 2.2 and supporting information Figure S1) reveals that RI locations separated by at least 24 hr in time can be considered as independent samples. Thus, the RI locations were also subsampled based on these considerations to ensure robust results. The increase in RI magnitude in the CETA is nearly 3 knots per 24 hr and is statistically significant at the 95% level. However, a similar analysis performed for the WTA shows that the mean RI magnitude has not changed significantly in that region during the 30-year period. These results offer strong support for our previous conclusion, based on the 95th percentile trend, that the magnitude of RI increased in the CETA during the 30-year period 1986–2015. Note that for both the WTA and CETA, the mean initial intensities of hurricanes at the RI locations were statistically indifferent

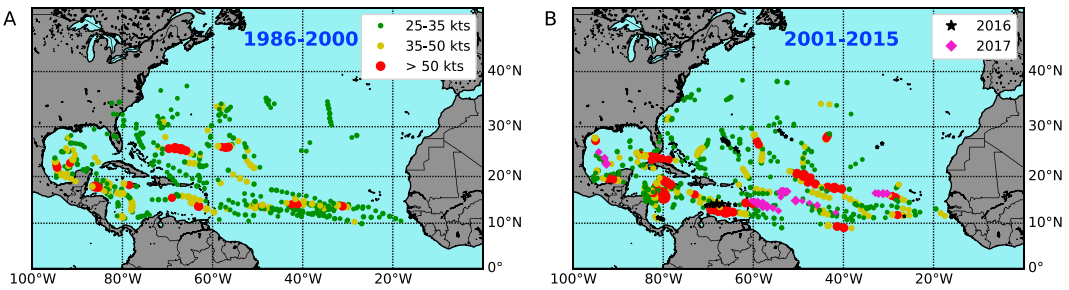

Figure 2. Hurricane track locations where rapid intensification (RI) occurred during (a) 1986–2000 and (b) 2001–2015. RI is defined as an intensity change of 25 knots or higher in 24 hr. Locations with RI magnitude between 25 and 35 knots are shown in green, between 35 and 50 knots are shown in yellow, and greater than 50 knots are shown in red. In panel (b), black stars indicate locations of RI during the 2016 hurricane season. Locations denoted by magenta diamonds are where hurricanes Harvey, Irma, Jose, and Maria underwent RI during the recent 2017 hurricane season.

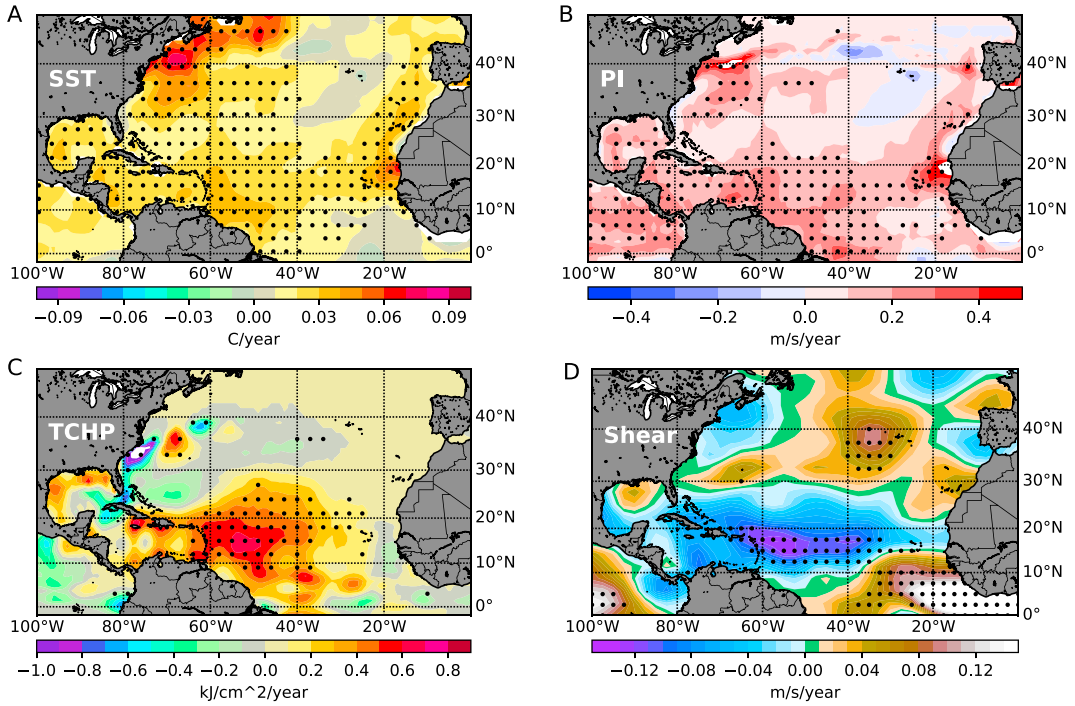

Figure 3. Trends in August–October averaged (a) sea surface temperature (SST) (°C/year), (b) potential intensity (PI; $m \cdot s^{-1} \cdot year^{-1}$), (c) tropical cyclone heat potential (TCHP; $kJ \cdot cm^{-2} \cdot year^{-1}$), and (d) vertical wind shear (VWS; $m \cdot s^{-1} \cdot year^{-1}$) over the 30-year period 1986-2015. Black dots indicate locations where the trends are statistically significant at the 95% level. SST trends are based on National Oceanic and Atmospheric Administration SST, trends in TCHP are based on Hadley EN4 subsurface oceanic temperature data, PI trends are based on National Oceanic and Atmospheric Administration SST and National Centers for Environmental Prediction-2 atmospheric reanalysis data, and VWS trends are based on National Centers for Environmental Prediction-2 atmospheric reanalysis data.

for the two 15-year periods. Further, a trend analysis performed for the probability of RI occurrence (supporting information Figure S2) indicates that there are no long-term changes in RI occurrence rates for the WTA nor CETA, consistent with previous studies (C. Wang et al., 2017).

3.2. Changes in Large-Scale Environment That Supports Hurricane RI

Having established that the magnitude of hurricane RI has increased in the CETA, we investigate the cause by examining changes in the hurricane environment over the months of August–October and for the same 30-year satellite period of 1986–2015 (see section 2.2). RI is affected by an interplay of the large-scale environmental parameters that typically govern hurricane intensification and decay (Kowch & Emanuel, 2015). The environmental parameters that have been identified to play a role in RI are SST, PI, TCHP, VWS evaluated between the 850- and 200-hPa pressure levels, 200-hPa divergence, relative humidity at 500 hPa, and cloud-top brightness temperature, for which we use outgoing longwave radiation as a proxy (Kaplan & DeMaria, 2003; Kaplan et al., 2010; C. Wang et al., 2017). During 1986–2015, SST increased over a broad region in the North Atlantic (Figure 3a), with the strongest warming centered in three regions. The first is located to the east of the Caribbean Sea and the islands of the Lesser Antilles between 60°W and 40°W and to the south of 20°N. The second is located near the African coast at about 20°W and 20°N and extends westward and northward. The third, less relevant for this study, is found to the north of 40°N hugging the U.S. and Canadian coasts and extending northward. The area-averaged trends in the CETA and WTA are 0.25°C per decade and 0.22°C per decade, respectively. These trends are significant at the 95% level. Unless otherwise noted, all trends mentioned hereafter are statistically significant at the 95% level. The spatial pattern of trends in PI is similar to that of SST, indicating that changes in PI are largely driven by those in SST (Figure 3b). The PI trend in the CETA is 1.8 ms^{-1} per decade and is slightly larger than in the WTA, where it is 1.5 ms^{-1} per decade. Unlike SST and PI, increases in TCHP show a strong peak in the CETA (Figure 3c). TCHP, a measure of the heat content in the upper ocean, increased substantially in the region to the east of the islands of Lesser Antilles between 60°W and 40°W and to the south of 30°N. A combination of SST increase (Figure 3a) and a deepening of the thermocline, defined as the depth of the 26°C isotherm (not shown), gives rise to the sharp

TCHP increase in this region. As a result, averaged over the CETA, the trend in TCHP is 2.9 kJ/cm^2 per decade. Despite an increase in a few small and isolated regions in the Caribbean Sea and the northern Gulf of Mexico, the area-averaged TCHP trend is statistically insignificant in the WTA. Thus, changes in the upper ocean more strongly favor an increase in RI magnitude in the CETA compared to the WTA. Next we consider changes in atmospheric conditions.

VWS displays a decreasing trend in much of the hurricane main development region in the CETA (Figure 3d). The strongest decreasing trends are found between 10°N and 20°N and approximately between 30°W and the eastern edge of the Caribbean Sea. When averaged over the CETA, the trend in VWS is -0.44 ms^{-1} per decade. On the other hand, trends in VWS in the WTA are not significant. Similarly, changes in upper-level divergence tend to enhance RI magnitude in the CETA (see SI). Positive divergence trends are found near the African coast between 10°N and 20°N and extending westward to 50°W. Averaged over the CETA, the trend in 200-hPa divergence is 2.6×10^{-7} s^{-1} per decade. In the Caribbean Sea, centered at about 80°W and 12°N, trends in upper-level divergence are strongly negative. As a result, when averaged over the WTA, the trend in 200-hPa divergence is -1.9×10^{-7} s^{-1} per decade. Finally, changes in relative humidity and outgoing longwave radiation are not significant in either subregion (not shown).

To further understand the role of these environmental parameters in RI magnitude changes, we performed a multivariate linear regression with the area-averaged time series of the parameters as predictors and the time series of 95th percentile of 24-hr intensity changes as the predictand. For the CETA, the variance explained by the linear model is nearly 40% and is significant at the 95% level based on the *F* test. The variance explained by these environmental parameters for the WTA is about 5% and is statistically insignificant. The apparent lack of control of the large-scale environmental parameters on the RI magnitude time series in the WTA is likely due to the dependence of RI in this region on atmospheric variability on short time scales, synoptic-scale weather systems, hurricane internal processes, and small-scale features in the climate system, such as mesoscale oceanic eddies in the Gulf of Mexico and the Caribbean Sea (Bosart et al., 2000; Mainelli et al., 2008; Shay et al., 2000; Scharroo et al., 2005; C. Wang et al., 2017).

Based on these results, which are independent of the specific data sources (supporting information Figure S3), we conclude that changes in the large-scale hurricane environment preferably favored an increase in RI magnitude in the CETA. This leads us naturally to the following question: What caused these changes in the environmental parameters? Atlantic hurricane activity is modulated at interannual to decadal time scales by climate phenomena such as the ENSO (Gray, 1984; Pielke & Landsea, 1999), the NAO (Elsner et al., 2000; Elsner, 2003; Kossin et al., 2010), the AMO (Goldenberg et al., 2001; Klotzbach & Gray, 2008; Trenberth & Shea, 2006), and the AMM (Kossin & Vimont, 2007; Vimont & Kossin, 2007). Among these four, only the AMO and AMM display significant trends for the period 1986–2015. The August–October averaged AMO and AMM indices have statistically significant trends of 0.127°C per decade and 1.28 per decade, respectively. On the other hand, trends in August–October averaged ENSO index and January–March averaged NAO index are insignificant. The positive trend in the AMO has been noted in previous studies (Sutton & Dong, 2012). Area-averaged time series of SST, PI, TCHP, VWS, and 200-hPa divergence are each significantly correlated at more than the 95% level with the time series of 95th percentile of 24-hr intensity changes in the CETA. However, when the influence of the AMO is removed from the various parameters, none is significantly correlated with the quantile time series except for divergence (Figure 4a). This suggests that part of the increase in upper-level divergence may be a direct consequence of the enhanced hurricane activity in the CETA region. But even for divergence, when the influence of the AMO is removed, the variance explained reduces substantially from 23.4% to 8.7%. This shows the important impact of the AMO on the factors that influence RI magnitude. The spatial pattern of the AMO index regressed onto SST (Figure 4b) is strikingly similar to the pattern of SST trends (Figure 3a), further emphasizing the role of the AMO. The decrease in VWS over the hurricane main development region to the east of the Caribbean Sea (Goldenberg et al., 2001; Knight et al., 2006; Shapiro & Goldenberg, 1998; Zhang & Delworth, 2006) and the increase in upper-level divergence in the eastern tropical Atlantic (Sun et al., 2017) are also consistent with atmospheric circulation changes induced by AMO.

Although the AMM also displays a statistically significant positive trend, its evolution is tightly linked to that of the AMO. Both the AMO (supporting information Figure S4a) and the AMM (supporting information Figure S4b) enter into predominantly positive phases over the second half of the 30-year period 1986–2015, and the two indices are strongly correlated at 0.82 (supporting information Figure S4c). This is consistent with Vimont and Kossin (2007), who show that the AMO is the primary driver of the AMM at decadal time scales. To

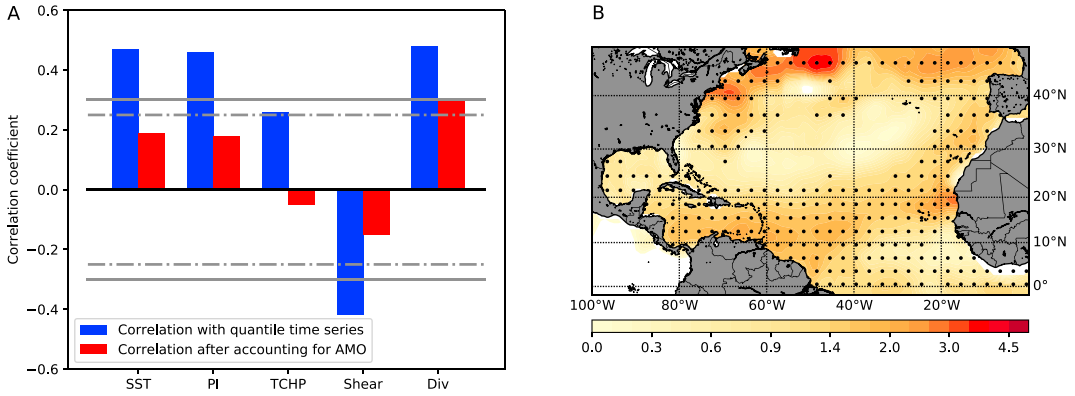

Figure 4. (a) Correlation coefficients for various environmental parameters with the time series of the 95th percentile of 24-hr intensity changes are shown in blue. The parameters have been averaged over the months August–October and over the central and eastern tropical Atlantic region. Correlation coefficients for the parameters with the quantile time series but with the influence of Atlantic Multidecadal Oscillation (AMO) removed from those parameters are shown in red. The dashed and solid gray lines denote statistical significance at the 90% and 95% levels, respectively. (b) Slope of linear regression between August–October averaged AMO index and August–October averaged sea surface temperature. Black dots denote regions where the regression coefficients are statistically significant at the 95% level.

understand the potential role of the AMM in RI magnitude increases in CETA, we performed correlation analysis between the various climate parameters that play a role in RI and the time series of the 95th percentile of 24-hr intensity changes in the CETA (supporting information Figure S5). The variance explained by these various parameters in the quantile time series is significantly reduced after accounting for the AMO, as noted previously. However, when the influence of AMM is additionally removed from these parameters, the variance explained does not change significantly. These results suggest that the impact of the AMM on the hurricane environment is not independent of the AMO's influence, in agreement with Vimont and Kossin (2007). Thus, we speculate that the AMO was the primary driver of the increase in mean RI magnitude in the CETA region, directly through its effect on the hurricane environment and indirectly through its influence on the AMM.

4. Discussion

Past studies have examined changes in Atlantic hurricane frequency, intensity, and overall activity (Elsner et al., 2008; Emanuel, 2005; Knutson et al., 2010; Sobel et al., 2016; Webster et al., 2005). However, changes in upper quantiles of intensification rates or the magnitude of RI have not been explored except for land-falling hurricanes in the Gulf of Mexico under future warming scenarios (Emanuel, 2017a). Our results, which demonstrate an increasing trend in RI magnitude in the CETA over the past three decades, have considerable societal relevance, particularly for the Caribbean islands that remain vulnerable to the devastating impacts of intense hurricanes (Pielke et al., 2003). While previous studies have suggested an increase in the overall hurricane activity as the main cause for an increase in the number of major hurricanes during the positive phase of the AMO (Goldenberg et al., 2001), by analyzing quantiles of 24-hr intensity change, we demonstrate that an increase in intense hurricanes can also occur due to an increase in RI magnitude without a change in Atlantic hurricane frequency.

Although we have attributed much of the increase in RI magnitude in the CETA to changes in the large-scale hurricane environment induced by a shift in the AMO, the role of anthropogenic climate change cannot be ruled out. When considering trends in SST based on the CMIP5 multimodel mean (supporting information Figure S6a), we note that the spatial pattern is broadly similar to that found in observations (Figure 3a). A pattern correlation performed between the spatial map of SST trends found in observations with that simulated by climate models yields a coefficient of 0.39, a value significant at the 90% level. However, trends in VWS simulated by the CMIP5 multimodel mean (supporting information Figure S6b) do not agree with those found in observations (Figure 3d). The models project an increase in VWS over much of the Caribbean Sea and near the western edge of the CETA region, consistent with previous studies on the impact of global warming on Atlantic hurricanes (Knutson et al., 2013; Vecchi & Soden, 2007). Hence, considering the disagreement between the spatial patterns of trends in VWS between observations and models, we suggest a lesser role for global warming in RI magnitude increases in the CETA. Despite this, studies have shown that it can be difficult

to isolate the role of the AMO from that of global warming when diagnosing tropical Atlantic SST variability (Mann et al., 2014; Mann & Emanuel, 2006). Further studies are needed to separate the influences of natural variability and climate change on the large-scale hurricane environment in the tropical Atlantic.

Although the AMO is currently in a positive phase, driving hurricane intensification, its future is not entirely clear. While some studies have suggested an amplification of the AMO signal under climate change (Moore et al., 2017), others indicate that we are on the verge of entering a negative AMO phase (Frajka-Williams et al., 2017; McCarthy et al., 2015). Given the serious implications of a continued increase in the magnitude of hurricane RI in the CETA region, our study emphasizes the need for a better understanding of the AMO and its future.

Acknowledgments
K. B. and L. R. L. were supported by the Office of Science (BER), U.S. Department of Energy as part of the Regional and Global Climate Modeling (RGCM) Program. The Pacific Northwest National Laboratory is operated for DOE by Battelle Memorial Institute under contract DE-AC05-76RL01830. G. F. was funded by base funds to NOAA/AOML's Physical Oceanography Division. The sources for various data used in this study are provided in section 2.

References

Behringer, D., & Xue, Y. (2004). Evaluation of the global ocean data assimilation system at NCEP: The Pacific Ocean. In *Proc. Eighth Symp. on Integrated Observing and Assimilation Systems for Atmosphere, Oceans, and Land Surface* (pp. 11–15). Seattle, Washington.

Bosart, L. F., Bracken, W. E., Molinari, J., Velden, C. S., & Black, P. G. (2000). Environmental influences on the rapid intensification of hurricane opal (1995) over the Gulf of Mexico. *Monthly Weather Review*, *128*(2), 322–352.

Chiang, J. C., & Vimont, D. J. (2004). Analogous Pacific and Atlantic Meridional Modes of tropical atmosphere–ocean variability. *Journal of Climate*, *17*(21), 4143–4158.

Dee, D. P., Uppala, S., Simmons, A., Berrisford, P., Poli, P., Kobayashi, S., et al. (2011). The ERA-interim reanalysis: Configuration and performance of the data assimilation system. *Quarterly Journal of the Royal Meteorological Society*, *137*(656), 553–597.

Elsberry, R. L. (2014). Advances in research and forecasting of tropical cyclones from 1963–2013. *Asia-Pacific Journal of Atmospheric Sciences*, *50*(1), 3–16.

Elsner, J. B. (2003). Tracking hurricanes. *Bulletin of the American Meteorological Society*, *84*(3), 353–356.

Elsner, J. B., Jagger, T., & Niu, X.-F. (2000). Changes in the rates of North Atlantic major hurricane activity during the 20th century. *Geophysical Research Letters*, *27*(12), 1743–1746.

Elsner, J. B., Kossin, J. P., & Jagger, T. H. (2008). The increasing intensity of the strongest tropical cyclones. *Nature*, *455*(7209), 92.

Emanuel, K. (2005). Increasing destructiveness of tropical cyclones over the past 30 years. *Nature*, *436*(7051), 686.

Emanuel, K. (2017a). Will global warming make hurricane forecasting more difficult? *Bulletin of the American Meteorological Society*, *98*(3), 495–501.

Emanuel, K. (2017b). Assessing the present and future probability of Hurricane Harvey's rainfall. *Proceedings of the National Academy of Sciences*, *114*(48), 12,681–12,684. https://doi.org/10.1073/pnas.171622211411207-011-9776-8

Emanuel, K. A. (1999). Thermodynamic control of hurricane intensity. *Nature*, *401*(6754), 665.

Frajka-Williams, E., Beaulieu, C., & Duchez, A. (2017). Emerging negative Atlantic Multidecadal Oscillation index in spite of warm subtropics. *Scientific Reports*, *7*(1), 11224.

Goldenberg, S. B., Landsea, C. W., Mestas-Nuñez, A. M., & Gray, W. M. (2001). The recent increase in Atlantic hurricane activity: Causes and implications. *Science*, *293*(5529), 474–479.

Good, S. A., Martin, M. J., & Rayner, N. A. (2013). EN4: Quality controlled ocean temperature and salinity profiles and monthly objective analyses with uncertainty estimates. *Journal of Geophysical Research: Oceans*, *118*, 6704–6716. https://doi.org/10.1002/2013JC009067

Gray, W. M. (1984). Atlantic seasonal hurricane frequency. Part I: El niño and 30 mb quasi-biennial oscillation influences. *Monthly Weather Review*, *112*(9), 1649–1668.

Hurrell, J. W. (1995). Decadal trends in the North Atlantic Oscillation: Regional temperatures and precipitation. *Science*, *269*(5224), 676–679.

Kanamitsu, M., Ebisuzaki, W., Woollen, J., Yang, S.-K., Hnilo, J., Fiorino, M., & Potter, G. (2002). NCEP–DOE AMIP-II reanalysis (r-2). *Bulletin of the American Meteorological Society*, *83*(11), 1631–1643.

Kaplan, J., & DeMaria, M. (2003). Large-scale characteristics of rapidly intensifying tropical cyclones in the North Atlantic basin. *Weather and Forecasting*, *18*(6), 1093–1108.

Kaplan, J., DeMaria, M., & Knaff, J. A. (2010). A revised tropical cyclone rapid intensification index for the Atlantic and eastern North Pacific basins. *Weather and Forecasting*, *25*(1), 220–241.

Klotzbach, P. J. (2012). El ni no-Southern Oscillation, the Madden-Julian Oscillation and Atlantic basin tropical cyclone rapid intensification. *Journal of Geophysical Research*, *117*, D14104. https://doi.org/10.1029/2012JD017714

Klotzbach, P. J., & Gray, W. M. (2008). Multidecadal variability in North Atlantic tropical cyclone activity. *Journal of Climate*, *21*(15), 3929–3935.

Knight, J. R., Folland, C. K., & Scaife, A. A. (2006). Climate impacts of the Atlantic Multidecadal Oscillation. *Geophysical Research Letters*, *33*, L17706. https://doi.org/10.1029/2006GL026242

Knutson, T. R., McBride, J. L., Chan, J., Emanuel, K., Holland, G., Landsea, C., et al. (2010). Tropical cyclones and climate change. *Nature Geoscience*, *3*(3), 157.

Knutson, T. R., Sirutis, J. J., Vecchi, G. A., Garner, S., Zhao, M., Kim, H.-S., et al. (2013). Dynamical downscaling projections of twenty-first-century Atlantic hurricane activity: CMIP3 and CMIP5 model-based scenarios. *Journal of Climate*, *26*(17), 6591–6617.

Kossin, J. P., & Vimont, D. J. (2007). A more general framework for understanding Atlantic hurricane variability and trends. *Bulletin of the American Meteorological Society*, *88*(11), 1767–1781.

Kossin, J. P., Camargo, S. J., & Sitkowski, M. (2010). Climate modulation of North Atlantic hurricane tracks. *Journal of Climate*, *23*(11), 3057–3076.

Kowch, R., & Emanuel, K. (2015). Are special processes at work in the rapid intensification of tropical cyclones? *Monthly Weather Review*, *143*(3), 878–882.

Landsea, C., Franklin, J., & Beven, J. (2015). The revised Atlantic hurricane database (HURDAT2), national hurricane center rep. 6 pp.

Lee, C.-Y., Tippett, M. K., Sobel, A. H., & Camargo, S. J. (2016). Rapid intensification and the bimodal distribution of tropical cyclone intensity. *Nature Communications*, *7*, 10625.

Leipper, D. F., & Volgenau, D. (1972). Hurricane heat potential of the Gulf of Mexico. *Journal of Physical Oceanography*, *2*(3), 218–224.

Mainelli, M., DeMaria, M., Shay, L. K., & Goni, G. (2008). Application of oceanic heat content estimation to operational forecasting of recent Atlantic category 5 hurricanes. *Weather and Forecasting*, *23*(1), 3–16.

Mann, M. E., & Emanuel, K. A. (2006). Atlantic hurricane trends linked to climate change. *Eos, Transactions American Geophysical Union*, *87*(24), 233–241.
Mann, M. E., Steinman, B. A., & Miller, S. K. (2014). On forced temperature changes, internal variability, and the AMO. *Geophysical Research Letters*, *41*, 3211–3219. https://doi.org/10.1002/2014GL059233
Masson, D., & Knutti, R. (2011). Climate model genealogy. *Geophysical Research Letters*, *38*, L08703. https://doi.org/10.1029/2011GL046864
McCarthy, G. D., Haigh, I. D., Hirschi, J. J.-M., Grist, J. P., & Smeed, D. A. (2015). Ocean impact on decadal Atlantic climate variability revealed by sea-level observations. *Nature*, *521*(7553), 508.
Meehl, G. A., Teng, H., & Arblaster, J. M. (2014). Climate model simulations of the observed early-2000s hiatus of global warming. *Nature Climate Change*, *4*(10), 898.
Moore, G., Halfar, J., Majeed, H., Adey, W., & Kronz, A. (2017). Amplification of the Atlantic Multidecadal Oscillation associated with the onset of the industrial-era warming. *Scientific Reports*, *7*, 40861.
Pielke, R. A., Jr., & Landsea, C. N. (1999). La Niña, El Niño and Atlantic hurricane damages in the united states. *Bulletin of the American Meteorological Society*, *80*(10), 2027–2033.
Pielke, R. A., Jr., Rubiera, J., Landsea, C., Fernández, M. L., & Klein, R. (2003). Hurricane vulnerability in Latin America and the Caribbean: Normalized damage and loss potentials. *Natural Hazards Review*, *4*(3), 101–114.
Rahmstorf, S. (2017). Rising hazard of storm-surge flooding. *Proceedings of the National Academy of Sciences*, *114*(45), 11,806–11,808.
Rappaport, E. N., Jiing, J.-G., Landsea, C. W., Murillo, S. T., & Franklin, J. L. (2012). The joint hurricane test bed: Its first decade of tropical cyclone research-to-operations activities reviewed. *Bulletin of the American Meteorological Society*, *93*(3), 371–380.
Rayner, N., Parker, D. E., Horton, E., Folland, C., Alexander, L., Rowell, D., et al. (2003). Global analyses of sea surface temperature, sea ice, and night marine air temperature since the late nineteenth century. *Journal of Geophysical Research*, *108*(D14), 4407. https://doi.org/10.1029/2002JD002670
Reynolds, R. W., Rayner, N. A., Smith, T. M., Stokes, D. C., & Wang, W. (2002). An improved in situ and satellite sst analysis for climate. *Journal of Climate*, *15*(13), 1609–1625.
Sampson, C. R., Kaplan, J., Knaff, J. A., DeMaria, M., & Sisko, C. A. (2011). A deterministic rapid intensification aid. *Weather and Forecasting*, *26*(4), 579–585.
Scharroo, R., Smith, W. H., & Lillibridge, J. L. (2005). Satellite altimetry and the intensification of Hurricane Katrina. *Eos, Transactions American Geophysical Union*, *86*(40), 366–366.
Shapiro, L. J., & Goldenberg, S. B. (1998). Atlantic sea surface temperatures and tropical cyclone formation. *Journal of Climate*, *11*(4), 578–590.
Shay, L. K., Goni, G. J., & Black, P. G. (2000). Effects of a warm oceanic feature on Hurricane Opal. *Monthly Weather Review*, *128*(5), 1366–1383.
Shu, S., Ming, J., & Chi, P. (2012). Large-scale characteristics and probability of rapidly intensifying tropical cyclones in the western North Pacific basin. *Weather and Forecasting*, *27*(2), 411–423.
Smith, T. M., Reynolds, R. W., & Ropelewski, C. F. (1994). Optimal averaging of seasonal sea surface temperatures and associated confidence intervals (1860–1989). *Journal of Climate*, *7*(6), 949–964.
Sobel, A. H., Camargo, S. J., Hall, T. M., Lee, C.-Y., Tippett, M. K., & Wing, A. A. (2016). Human influence on tropical cyclone intensity. *Science*, *353*(6296), 242–246.
Sun, C., Kucharski, F., Li, J., Jin, F.-F., Kang, I.-S., & Ding, R. (2017). Western tropical pacific multidecadal variability forced by the Atlantic Multidecadal Oscillation. *Nature Communications*, *8*, 15998.
Sutton, R. T., & Dong, B. (2012). Atlantic Ocean influence on a shift in european climate in the 1990s. *Nature Geoscience*, *5*(11), 788.
Trenberth, K. E., & Shea, D. J. (2006). Atlantic hurricanes and natural variability in 2005. *Geophysical Research Letters*, *33*, L12704. https://doi.org/10.1029/2006GL026894
Vecchi, G. A., & Soden, B. J. (2007). Increased tropical atlantic wind shear in model projections of global warming. *Geophysical Research Letters*, *34*, L08702. https://doi.org/10.1029/2006GL028905
Vimont, D. J., & Kossin, J. P. (2007). The Atlantic Meridional Mode and hurricane activity. *Geophysical Research Letters*, *34*, L07709. https://doi.org/10.1029/2007GL029683
Wang, B., & Zhou, X. (2008). Climate variation and prediction of rapid intensification in tropical cyclones in the western North Pacific. *Meteorology and Atmospheric Physics*, *99*(1-2), 1–16.
Wang, C., Wang, X., Weisberg, R. H., & Black, M. L. (2017). Variability of tropical cyclone rapid intensification in the North Atlantic and its relationship with climate variations. *Climate Dynamics*, *49*(11-12), 3627–3645.
Webster, P. J., Holland, G. J., Curry, J. A., & Chang, H.-R. (2005). Changes in tropical cyclone number, duration, and intensity in a warming environment. *Science*, *309*(5742), 1844–1846.
Wolter, K., & Timlin, M. S. (1998). Measuring the strength of ENSO events: How does 1997/98 rank? *Weather*, *53*(9), 315–324.
Zhang, R., & Delworth, T. L. (2006). Impact of Atlantic Multidecadal Oscillations on India/Sahel rainfall and Atlantic hurricanes. *Geophysical Research Letters*, *33*, L17712. https://doi.org/10.1029/2006GL026267
Zorrilla, C. D. (2017). The view from Puerto Rico—Hurricane Maria and its aftermath. *New England Journal of Medicine*, *377*(19), 1801–1803.